

# On the Structures and Yields of the First Peroxyl Radicals in $\gamma$ -Irradiated Polyolefins<sup>†</sup>

D. J. Carlsson,\* S. Chmela,<sup>‡</sup> and J. Lacoste<sup>§</sup>

Division of Chemistry, National Research Council of Canada,  
Ottawa, Ontario, Canada K1A 0R9

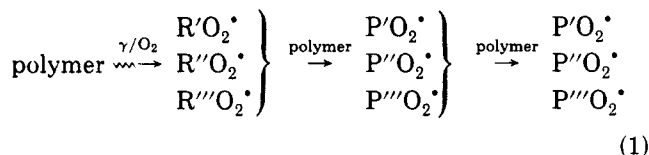
Received February 14, 1990

**ABSTRACT:** Peroxyl radicals generated as a result of  $\gamma$ -irradiation of isotactic and atactic polypropylene and high-density polyethylene have been identified and quantified by a combination of electron spin resonance (ESR) and derivitization infrared spectroscopies. When samples are maintained at  $\leq -60^\circ\text{C}$ , peroxyl radicals are indefinitely stable in polyolefins yet react smoothly with nitric oxide to give nitrates. From infrared spectroscopy it is possible to identify the structure of some of these nitrates (primary, secondary, or tertiary) and hence the structure of the peroxyl radicals that are the origin of all oxidative chains in the polymers. Good agreement was found between total peroxyl species measured by ESR and the total level of nitrate products from infrared. From polyethylene, the dominant peroxyl species is proposed to be  $\sim\text{CH}_2\text{CH}(\text{O}_2^\bullet)\text{-CH}_2\sim$ , whereas in the polypropylenes the secondary peroxyl dominated over the tertiary species. This dominance is very different from that expected from peroxyl radical selectivity for attack on polymer CH groups in the subsequent propagation reactions.

## Introduction

High-energy radiations ( $\gamma$ - or X-rays or electron beams) provide a convenient source of free radicals in polyolefins for the study of their oxidation mechanisms.<sup>1-3</sup> In addition, plastic medical equipment is readily sterilized by these radiations, but the extensive polymer degradation during both exposure and subsequent storage is a major practical problem for this process.<sup>4</sup> Several studies have attempted to interpret the electron spin resonance (ESR) spectra of irradiated polyolefins in terms of the carbon-centered radicals produced by radiation.<sup>2,5-7</sup> Most studies employed irradiation at very low temperatures in an attempt to freeze-out the subsequent reactions of the initial radicals.

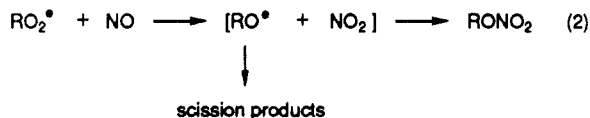
For the oxidative degradation of polymers, the identification of the initial peroxyl radicals that actually begin the oxidative chain processes is of much greater importance than the nature of the macroalkyl radical(s) produced by irradiation, especially if these result from abnormal conditions. It is very likely that the first peroxyl radicals produced by high-energy irradiation will not be typical of the normal peroxyl species produced by free-radical propagation reactions. In the former case, reactions of the ions and electrons produced by the radiation in the polymer will dictate the structure of the first peroxyl species ( $\text{RO}_2^\bullet$ ). In the latter case, the peroxyl radicals ( $\text{PO}_2^\bullet$ ) are controlled by the selectivity of abstraction reactions by the peroxyl radicals themselves and are repeatedly regenerated by the propagation processes (reaction 1).



Although ESR can allow the quantification of the free radicals in solid polymers, identification of their precise structure (primary, secondary, or tertiary, backbone or

chain end, etc.) is only possible for single alkyl species, complex for alkyl radical mixtures, and extremely difficult for peroxyl radicals. The fine structure of spin trap products from peroxyl-nitron reactions has been used to identify peroxyl species in the liquid phase, although the adducts are quite unstable.<sup>8</sup> Broadening of ESR spectra and slow diffusive penetration in the solid preclude the use of this method for irradiated polyolefins. Peroxyl radicals from small alkyls have been observed directly in the IR by matrix isolation, but macroperoxyl radicals could not be directly observed in polymers.<sup>3</sup>

We have recently developed a method based on infrared (IR) spectroscopy for the identification and quantification of primary, secondary, and tertiary hydroperoxides.<sup>10,11</sup> This method depends upon their conversions to the corresponding nitrates by reaction with nitric oxide, which can diffuse through the solid polymer as readily as oxygen. The IR spectra of these nitrates are distinctive of the precise structure of the alkyl substituent and have intense IR absorptions. Volatile peroxyl radicals ( $\text{RO}_2^\bullet$ ) have been shown to react very rapidly with NO to give nitrates in photochemical smogs (reaction 2).<sup>12</sup> In this paper we discuss the potential of using this NO reaction for the identification of macroperoxyl radicals produced by  $\gamma$ -irradiation of polypropylene and polyethylene.



## Experimental Section

Isotactic polypropylene films (i-PP, Himont Profax, 25  $\mu\text{m}$ ) and high-density polyethylene films (PE, Union Carbide, 0.958 g/mL density, <0.1 methyl/100 carbons, 25  $\mu\text{m}$ ) were acetone extracted for 48 h to remove processing antioxidants and then vacuum-dried. Atactic polypropylene (a-PP, Hercules experimental resin, zero crystallinity by DSC, zero helical content by infrared) was cast from toluene into thin films on glass. These pliable, but tack-free films could be stripped from the glass after chilling and then handled in essentially the same way as the i-PP and PE films.

Films were exposed to  $\gamma$ -irradiation (AECL Gamma Cell 220, dose rate 0.77 Mrad/h) under air, oxygen, or vacuum at  $-196^\circ$  or  $-78^\circ\text{C}$  (dry ice). Samples for ESR studies were rolled into

<sup>†</sup> Issued as NRCC No. 32496.

<sup>‡</sup> Research Associate, 1986-1988. Permanent address: Polymer Institute, Slovak Academy of Science, Bratislava, Czechoslovakia.

<sup>§</sup> Guest Researcher. Permanent address: Université Blaise-Pascal, Clermont-Ferrand, France.

scrolls designed to slide easily into 5.0-mm-o.d. ESR tubes after irradiation. Irradiated scrolls were dropped into liquid nitrogen before loading into fresh ESR tubes, also cooled to  $-196^\circ\text{C}$  so that no loss of radicals occurred. The ESR spectra were recorded at various microwave power settings on a Varian E4 X-band spectrometer coupled to an Apple computer for data storage and subsequent double integration as described previously.<sup>13</sup> Absolute radical yields were estimated by comparison with either a cupric acetylacetonate standard or a galvinoxyl standard, both prepared by gravimetry after dilution with pure powdered KCl. These standards both obeyed the Curie law over the ambient to  $-150^\circ\text{C}$  range (in contrast to other standards such as nitroxides, DPPH, etc.). All radical yields were measured from ESR spectra recorded on samples cooled to  $-140$  to  $-120^\circ\text{C}$ .

Some of our previously published peroxy radical concentrations depended on the use of DPPH in benzene.<sup>13</sup> Deviations from Curie law behavior on cooling to  $-150^\circ\text{C}$  imply radical-radical association to give erroneously low signals and consequently low estimates of absolute peroxy radical concentrations. Relative concentrations are however still valid.

Films for infrared analysis were irradiated as flat  $2 \times 1$  cm strips which were transferred cold into the traplike NO-treatment cell held at  $-78^\circ\text{C}$ .<sup>10</sup> After the cell was purged with  $\text{N}_2$ , chilled by passage through a cooling coil in dry ice, for  $\sim 15$  min to remove all  $\text{O}_2$ , NO (Matheson) was passed through the cooling coil into the cell for  $\sim 5$  min, and then the film samples were isolated in the NO atmosphere for up to 20 h at  $-78^\circ\text{C}$  by closing the entrance and exit valves. Throughout this treatment the irradiated films were maintained at  $\leq -78^\circ\text{C}$ . After NO exposure, the large excess of NO was swept out with  $\text{N}_2$  to prevent  $\text{NO}_2$  formation around the samples by reaction with atmospheric oxygen. Films were examined by Fourier transform IR (FTIR, Perkin-Elmer 1500) after tilting at the Brewster angle and by using a gold-wire-grid polarizer to eliminate the formation of interference ripples in the spectra.<sup>14</sup> Usually four identical films were plied together to improve the detection of NO reaction products. Spectral subtractions using the dedicated computer of the FTIR were performed to emphasize changes.

The rates of the reaction of NO with peroxy radicals in PP and PE were examined by ESR spectroscopy on irradiated film scrolls held at  $-78 \pm 10^\circ\text{C}$  in the spectrometer. After the initial peroxy signal was recorded, NO was admitted via a break seal to the preevacuated sample, and spectra were recorded periodically as the peroxy signal decayed.

## Results and Discussion

The radicals produced by  $\gamma$ -irradiation of polyolefins can be quantified and classified into broad categories by ESR spectroscopy. At  $-140^\circ\text{C}$ , the anisotropic signal from irradiated i-PP and a-PP is typical of peroxy and shows no additional features attributable to alkyl species (Figure 1A). At this temperature the signal indicates the presence of a nonrotating peroxy site.<sup>15,16</sup> The small ripples visible in the wings of the ESR spectra of the PE samples result from macroalkyl radicals. Upon warming to room temperature, the peroxy radicals in a-PP, i-PP, and PE decay quite quickly but show the typical line shapes shown in Figure 1B. Both signals indicate rotation of the peroxy site, with rapid rotation in the case of PE.<sup>15</sup>

$\gamma$ -Irradiation at  $-196^\circ\text{C}$  in oxygen produces a mixture of peroxy and macroalkyl radicals from both i-PP and PE. Storage at  $-78^\circ\text{C}$  in the presence of oxygen causes alkyl to peroxy conversion over 10–15 h to give spectra identical with those shown in Figure 1. Prolonged storage in oxygen at  $-78^\circ\text{C}$  causes no further loss of the alkyl features in the PE spectrum. These features may indicate trapped macroalkyl sites in the oxygen-impermeable crystalline domains in PE. For melt-quenched i-PP the crystalline phase is probably completely permeable to oxygen so that only peroxy radicals are detected.<sup>16</sup>

For a given radiation dose, the total radical yields as measured by double integration were found to be identical

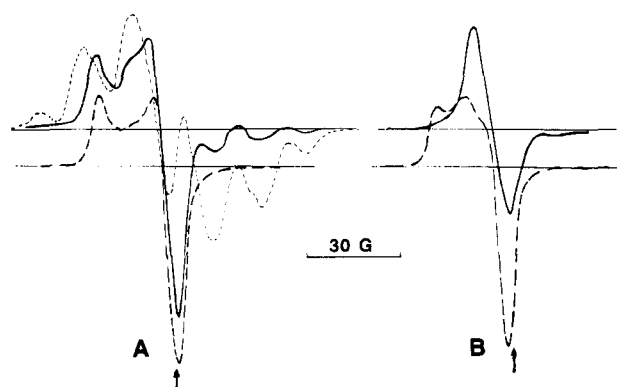


**Figure 1.** Polyolefin ESR spectra after  $\gamma$ -irradiation (1.0-Mrad dose and 0.5-mW microwave power). (A) Spectra measured at  $-130^\circ\text{C}$ : (---) i-PP film irradiated at  $-78^\circ\text{C}$  in air; (—) PE film irradiated at  $-78^\circ\text{C}$  in air; (---) PE film irradiated at  $-196^\circ\text{C}$  under vacuum. (B) Spectra measured at  $22^\circ\text{C}$  in air after  $\sim 1$  min at  $22^\circ\text{C}$ : (---) i-PP film irradiated as in (A); (—) PE film irradiated at  $-78^\circ\text{C}$  in air. Each arrow indicates  $g = 2.0036$  from DPPH calibration.

**Table I**  
Products from the  $\gamma$ -Irradiation of Polyolefins<sup>a</sup>

polyolefin	$[\text{R}^\bullet]^b$	$[\text{RO}_2^\bullet]^c$	primary $\text{RONO}_2^d$	secondary $\text{RONO}_2^d$	tertiary $\text{RONO}_2^d$
HDPE	$2.8 \pm 0.5$	$2.1 \pm 0.5^e$	0	$1.9 \pm 0.2$	0
i-PP	$3.6 \pm 0.5$	$3.5 \pm 0.5$	$0.3 \pm 0.1$	$1.7 \pm 0.2$	$0.9 \pm 0.2$
a-PP	ND	$3.2 \pm 0.5$	$0.4 \pm 0.1$	$1.6 \pm 0.2$	$0.7 \pm 0.2$

<sup>a</sup> All products in  $\times 10^3$  (mol/kg)/Mrad irradiation. Data normalized to products/Mrad for samples irradiated in the range 0.5–10-Mrad dose. <sup>b</sup> From ESR, irradiation under vacuum at  $-196^\circ\text{C}$ . <sup>c</sup> From ESR, irradiation under  $\text{O}_2$  or air at  $-78^\circ\text{C}$  followed by  $\sim 15$  h at  $-78^\circ\text{C}$  under  $\text{O}_2$  or air. Identical yield when vacuum-irradiated sample was exposed to  $\text{O}_2$  or air for  $\sim 15$  h at  $-78^\circ\text{C}$ . <sup>d</sup> From FTIR, after  $\text{RO}_2$  exposure to NO at  $-78^\circ\text{C}$ . <sup>e</sup> Also with  $(0.6 \pm 0.2) \times 10^{-3}$  mol/kg of trapped macroalkyl radicals.

for PE samples irradiated under vacuum at  $-196$  or  $-78^\circ\text{C}$ , after exposure of these samples to oxygen at  $-78^\circ\text{C}$ , or after irradiation at  $-78^\circ\text{C}$  in air. The same correspondence was found for a-PP and i-PP film samples, although the latter gave higher radical yields than PE (Table I).

The intensity of the ESR spectrum of a radical increases linearly with the half order of the microwave power applied up to a point where energy-level saturation begins.<sup>17</sup> From a study of the power saturation behavior of macroalkyl and peroxy radicals it is possible to derive the concentrations of both radicals in  $\gamma$ -irradiated PE. At  $\leq 0.5$ -mW microwave power for our system, both radicals contribute fully to the ESR signal. At 10 mW, only peroxy radicals contribute fully [signal  $\propto (\text{power})^{1/2}$ ], whereas macroalkyls contribute only 1.5 times their 0.5-mW value (plateauing at a power level of  $\sim 1.5$  mW). From the double-integration intensities at 0.5 and 10 mW, the total radical yield after 1.0-Mrad irradiation in air or in oxygen is  $(2.8 \pm 0.5) \times 10^{-3}$  mol/kg and is calculated to be made up of  $(2.1 \pm 0.5) \times 10^{-3}$  peroxy and  $(0.6 \pm 0.2) \times 10^{-3}$  alkyl species. The broad error limits result from the difficulties of making precise double integrations on both the irradiated polymer and the ESR standards. Identical macroalkyl to peroxy ratios were found for PE irradiated at  $-196^\circ\text{C}$  or  $-78^\circ\text{C}$  in air or  $\text{O}_2$  or under vacuum followed by  $\text{O}_2$  exposure at  $-78^\circ\text{C}$ .

Peroxy radicals from a-PP, i-PP, and PE do not decay at  $\leq -60^\circ\text{C}$  under vacuum, in air, or in  $\text{O}_2$  as observed by ESR. The absence of peroxy termination and propagation at  $\leq -60^\circ\text{C}$  was confirmed on films irradiated at  $-78^\circ\text{C}$ , followed by FTIR analysis on films held at  $\leq -60^\circ\text{C}$  in the

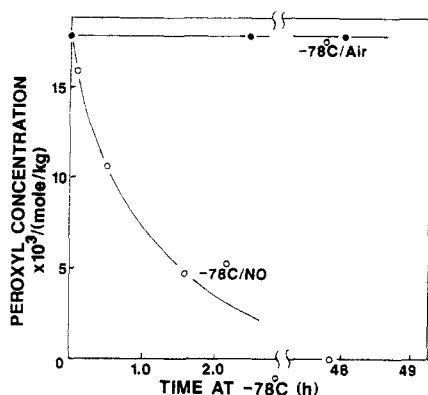


**Figure 2.** Peroxyl radical decay from ESR spectroscopy. PE film  $\gamma$ -irradiated to 6-Mrad dose in air and transferred for storage in air (closed symbols) or NO (open symbols). Samples maintained at  $\leq -78^\circ\text{C}$  throughout.

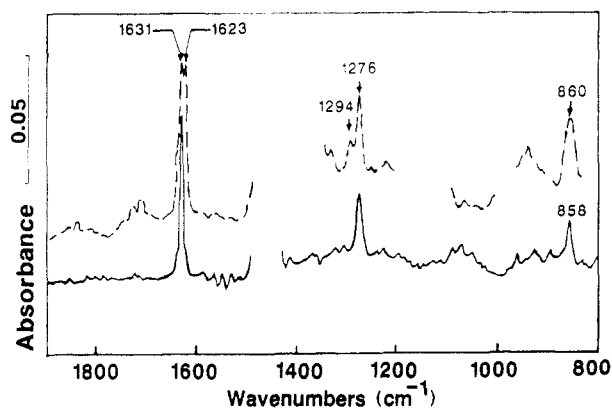


**Figure 3.** Nitrate products from peroxyl radicals by FTIR. All samples exposed to 6-Mrad  $\gamma$ -irradiation at  $-78^\circ\text{C}$  in air, followed by 5 h. NO exposure at  $-78^\circ\text{C}$ . Spectra obtained by subtracting the spectrum of the starting film from that of the treated film in all cases. (---) i-PP samples,  $4 \times 25 \mu\text{m}$  films; (—) PE samples,  $4 \times 25 \mu\text{m}$  films.

spectrometer.<sup>3</sup> Neither carboxyl species (at  $\sim 1718 \text{ cm}^{-1}$ , radical termination products) nor hydroxyl species at  $\sim 3400 \text{ cm}^{-1}$ , including OOH species from peroxyl propagation) were detected over several hours. These products do form within seconds of warming to room temperature.<sup>3</sup> Thus  $-78^\circ\text{C}$  represents the highest convenient temperature at which it should be possible to generate and characterize peroxyl radicals. It is proposed that these peroxyl radicals observed at  $-78^\circ\text{C}$  are representative of the species that begin the oxidative process following  $\gamma$ -irradiation at ambient temperature.

Although peroxyl radicals from a-PP, i-PP, and PE are indefinitely stable at  $-78^\circ\text{C}$ , peroxyl reaction with NO proceeded rapidly at this temperature with no detectable new radicals (Figure 2). After complete loss of radicals, the NO-exposed,  $\gamma$ -irradiated films had the FTIR changes shown in Figure 3. It is important to note the complete absence of carbonyl species ( $\sim 1715 \text{ cm}^{-1}$ ). This confirms that radical termination had not occurred as a result of accidental warming above  $-60^\circ\text{C}$  and that all of the  $\gamma$ -generated peroxyl radicals were available for reaction with NO.

In order to identify peroxyl-NO reaction products, FTIR spectra of many model nitrates were recorded in various environments (Table II). From these data, the nitrate peaks at  $1295\text{--}1276 \text{ cm}^{-1}$  (width at half-height  $\sim 12 \text{ cm}^{-1}$ ) can be used to differentiate tertiary nitrates (at  $1294 \text{ cm}^{-1}$ ) from secondary and primary nitrates (at  $1276 \text{ cm}^{-1}$ ). These absorptions are quite insensitive to the polarity of the

environment. The  $\sim 860\text{-cm}^{-1}$  peaks are not useful, being quite broad and overlapped for all nitrates. The sharp  $1640\text{--}1620\text{-cm}^{-1}$  absorptions (width at half-height  $\sim 8 \text{ cm}^{-1}$ ) are sensitive to polarity, moving to lower frequency with increasing local polarity (either from their solvent or from nitrate concentration). However, primary nitrates always absorbed at higher frequencies ( $1641\text{--}1635 \text{ cm}^{-1}$ ) than secondary or tertiary nitrates.

The two sharp peaks at  $1631$  and  $1623 \text{ cm}^{-1}$  from i-PP peroxyl reaction with NO (Figure 3) are tentatively assigned to isolated secondary and tertiary nitrate groups ( $1631 \text{ cm}^{-1}$ ) and clustered secondary and tertiary nitrate groups ( $1623 \text{ cm}^{-1}$ ), respectively. Here "clustered" is meant to imply nitrate groups (two or more) close enough to affect their IR spectra because of the polarity of their nitrate function. These assignments are based on peak locations in Table II, together with relative extinction coefficients at  $\sim 1631$ ,  $1623$ ,  $1276$ , and  $1294 \text{ cm}^{-1}$ .<sup>10</sup> Isolated nitrate groups are dominant in PE (Figure 3), the clustered absorption at  $1623 \text{ cm}^{-1}$  only becoming detectable at high doses ( $\geq 6 \text{ Mrad}$ , not shown). This is consistent with C-H scission by  $\gamma$ -irradiation followed by hydrogen abstraction by the hot  $\text{H}^\bullet$  from the initial scission at a site quite distant from this initial scission. In i-PP, the  $1623\text{-}$  and  $1630\text{-cm}^{-1}$  absorptions are close to equal and imply the presence of isolated peroxyl sites as are formed in PE, together with closely spaced sites. The latter may originate in part from the higher backbone rigidity (higher  $T_g$ ) of i-PP as compared to PE and consequently lower  $\text{H}^\bullet$  mobility before attack on the polymer. The twin IR peaks in i-PP are not related to crystallinity effects as exactly the same spectrum was found from a-PP (zero crystallinity). Furthermore, the twin peaks do not result from dinitrates such as 1,3-dinitrates. Models with these substituents absorbed at  $1646 \text{ cm}^{-1}$ .

From a comparison of the IR spectra of model nitrates and the peroxyl-NO reaction products from i-PP, a-PP, and PE, concentrations of the various species can be calculated (Table I). These concentrations have been calculated by using peak areas because changes in peak width accompany the shifts in peak position with environment, leading to a variation in height-based extinction coefficients. In addition, separation (deconvolution) of the overlapped peaks is necessary for quantification. This was effected by spectral subtraction of the simple secondary nitrate spectrum of PE from the more complex spectrum of  $\gamma$ -irradiated i-PP (Figure 3). This assumes, of course, that secondary nitrate groups in PE and in i-PP have identical spectra, which is only valid for the  $1300\text{--}1270\text{-cm}^{-1}$  region. The residual spectrum (not shown) showed the isolated  $1294\text{-cm}^{-1}$  peak of the tertiary nitrate groups in PP. The values in Table I are the averages of several experiments covering a range of  $0.5\text{--}20 \text{ Mrad}$ . Both radical levels from ESR and peroxyl levels from FTIR of their nitrate products were completely linear with increasing  $\gamma$ -dose over this range.

The peroxyl concentrations from ESR and the sum of peroxyl species from the FTIR method (Table I) are in fair agreement, bearing in mind the errors in absolute radical concentration measurement by ESR and in the FTIR method. This agreement indicates close to quantitative conversion of macropoxyl to nitrate under our reaction conditions ( $-78^\circ\text{C}$  in the solid polymer). This contrasts with the low conversion to nitrates ( $\sim 10\%$ ) reported for NO reaction with gaseous peroxyl radicals important in air pollution.<sup>12</sup> This low nitrate yield in the gas phase may be attributable to escape of volatile alkoxyl radical (from reaction 2) before combination to give nitrate.

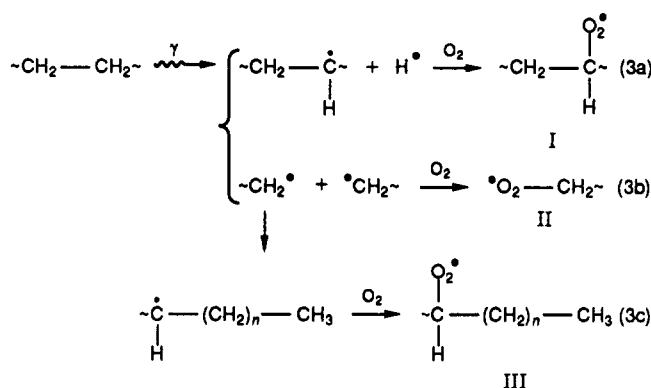
Table II  
IR Absorption Maxima for Model Nitrates

model nitrate	absorp max, $\text{cm}^{-1}$			environment
primary $\text{CH}_3(\text{CH}_2)_{10}\text{ONO}_2$ $\text{CH}_3\text{CH}_2\text{CH}(\text{CH}_2\text{ONO}_2)\text{CH}_2\text{CH}_3$	1641 1635	1278 1278	850 860	hexane <sup>a</sup> { $\text{CH}_3\text{CN}^a$ hexane <sup>b</sup>
secondary $\text{CH}_2(\text{CH}_2)_4\text{CH}(\text{ONO}_2)\text{CH}_2\text{CH}_3$ $\text{CH}_3(\text{CH}_2)_7\text{CH}(\text{ONO}_2)\text{CH}_3$ $\text{CH}_3\text{CH}(\text{CH}_3)\text{CH}(\text{ONO}_2)\text{CH}(\text{CH}_3)\text{CH}_3$ $\text{CH}_3\text{CH}(\text{CH}_3)\text{CH}_2\text{CH}(\text{ONO}_2)\text{CH}_2\text{CH}(\text{CH}_3)\text{CH}_2\text{CH}(\text{CH}_3)_2$	1633 1623	1276 1276	867-860 867-860	hexane <sup>a</sup> { hexane <sup>b</sup> $\text{CH}_3\text{CN}^a$ or Tornac <sup>c</sup>
tertiary $\text{CH}_3\text{C}(\text{CH}_3)_2\text{CH}_2\text{C}(\text{CH}_3)_2\text{ONO}_2$ $\text{CH}_3\text{CH}_2\text{C}(\text{CH}_3)(\text{ONO}_2)\text{CH}_2\text{CH}_3$	1630 1623	1294 1305, 1294	862 861	hexane <sup>a</sup> { hexane <sup>b</sup> $\text{CH}_3\text{CN}^a$

<sup>a</sup> Dilute solution,  $\sim 5 \times 10^{-3}$  mol/L. <sup>b</sup> Concentrated solution,  $\sim 2$  mol/L. <sup>c</sup> Hydrogenated, random butadiene-acrylonitrile copolymer.

The detected peroxy species can be compared with those expected by the  $\gamma$ -radiation cleavage of bonds in PE and PP.

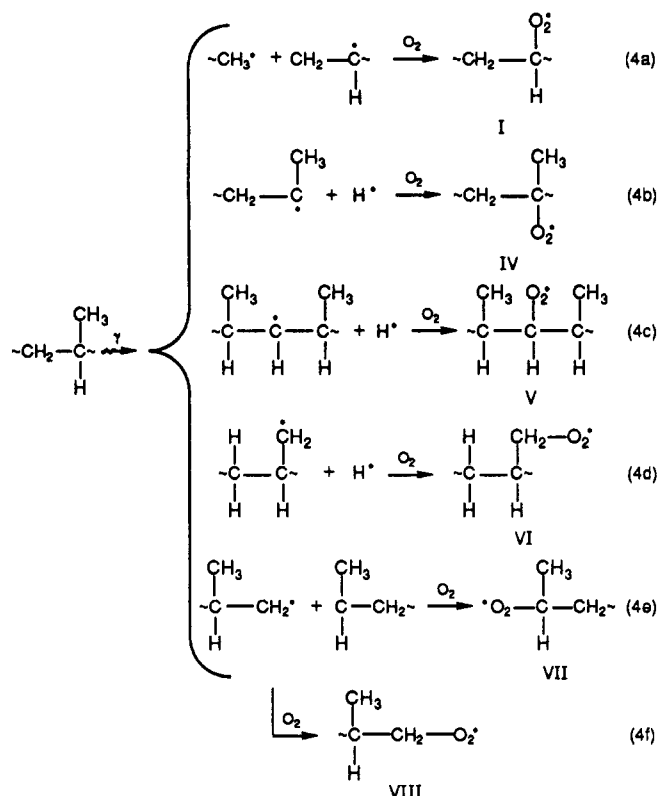
PE is obviously the simpler system and possible species (I and II) are shown in eq 3. Attack of any of the mac-



roalkyl radicals or  $\text{H}^\bullet$  on the surrounding PE chains will generate the macroalkyl radical, yielding peroxy I. Peroxy II would give a primary nitrate but was not detected. Although 1,2-H-atom shifts are unknown for alkyl radicals, intramolecular shifts, such as 1,6-H-atom transfer, are possible to give eventually peroxy III ( $n = 4$ ), as well as intermolecular H abstraction to give eventually peroxy radical I.<sup>18,19</sup> Both I and III would give indistinguishable secondary nitrates. However, H-atom transfer is slower than peroxy formation by a factor of ca.  $10^2$ .<sup>18,19</sup> Consequently, only the primary peroxy radical (and hence primary nitrate) should result from backbone scission (reaction 3b). Our failure to detect primary nitrate in  $\gamma$ -irradiated PE implies that this latter reaction is very rare or recombination very rapid.

i-PP and a-PP can potentially give a much more complex mix of alkyl radicals than PE (eq 4). Any of these macroalkyl radicals may undergo intra- or (less likely) intermolecular H-atom transfer prior to reaction with  $\text{O}_2$ .<sup>18</sup> These H-transfer processes will simply lead to peroxy radicals IV, V, and/or VI but probably cannot compete with  $\text{O}_2$  interception.<sup>18,19</sup>

Only trace amounts of methane have been reported from i-PP  $\gamma$ -irradiated in the absence of oxygen, hydrogen being by far the dominant gaseous product.<sup>20</sup> This precludes I as a significant product. The FTIR spectral features attributed to secondary nitrate can originate from peroxy V and/or VII. The tertiary nitrate species must come from IV, whereas the primary nitrate species may result from VI and/or VIII.



Although one initial objective had been to quantify peroxy radicals resulting from backbone scission and from loss of side groups ( $\text{H}^\bullet$  and  $\text{CH}_3^\bullet$  elimination), the shifts in the  $\sim 1630\text{-cm}^{-1}$  nitrate absorptions caused by the (possible) presence of isolated and clustered nitrate groups has made this extremely difficult. However, the very low yield of primary nitrate (Table I) attributable to nitrates VI and VIII implies that the backbone scission reaction is rare as compared to side-group ( $\text{H}^\bullet$ ) elimination. We have previously detected pendant carboxylic acid groups  $\{\sim\text{CH}_2\text{CH}[\text{C}(=\text{O})\text{OH}]\text{CH}_2\sim\}$  from the  $\gamma$ -initiated oxidation of i-PP.<sup>10</sup> These pendant acid groups from PP can most reasonably originate from reactions of primary peroxy radicals VI which may thus be the dominant component of the primary peroxy species observed (Table I).

The observed radical yields and tentative radical structures can be compared with previously published data, although much of this data was obtained at  $-196^\circ\text{C}$ . Our total radical yield from PE (Table I) is in good agreement with the  $G$  values reported by Dole for unoriented PE [ $G(\text{alkyl}) = 2.5 \pm 0.3$ , which gives a yield of  $2.5 \times 10^{-3}$  mol/kg for a 1 Mrad dose].<sup>5</sup> Both PE and i-PP give large yields

of H<sub>2</sub> upon  $\gamma$ -irradiation under vacuum ( $\sim 3.7 \times 10^{-3}$  and  $\sim 3 \times 10^{-3}$  mol/kg, respectively, for each Mrad dose).<sup>5,6</sup> Both polymers are reported to undergo some backbone chain scission but the reported values are the net result of a complex series of reactions following irradiation (dependent on temperature, time, precise conditions when exposed to air, etc.) rather than the direct  $\gamma$ -radiolysis effect. The large dominance of side-group C-H scission as compared to backbone C-C scission has been variously attributed to energy transfer, excited-state effects, or extensive recombination of macroalkyl radical pairs.<sup>21-23</sup> The complex, overlapped ESR spectra of macroalkyl radicals produced by irradiating PP at -196 °C under vacuum have been interpreted as those leading to peroxy radicals IV, VI, or V or combinations of these. Dole has identified the macroalkyl leading to peroxy VI as a dominant species at -196 °C but it converts to the macroalkyl leading to IV at ca. -70 °C in the absence of oxygen.<sup>17</sup>

In conclusion, the NO reaction products with peroxy radicals can be used to partially identify these radicals. From this method it is apparent that the  $\gamma$ -irradiation of PP produces an initial mix of peroxy radicals (Table I) very different from the relative concentrations expected from the selectivity of propagating peroxy radicals involved in the oxidation of the polymer (attack on primary: secondary:tertiary CH sites  $\sim 1:20:200$  for liquid model hydrocarbons).<sup>24</sup> The atypical mixture (Table I) is consistent with the high yield of secondary hydroperoxides as compared to tertiary found from  $\gamma$ -oxidized PP containing highly effective stabilizer systems that suppress both the propagation of the initial peroxy radicals and prevent loss of physical properties.<sup>21</sup>

**Acknowledgment.** We are grateful to a referee for guidance on the possible interconversion of alkyl radicals.

## References and Notes

- (1) Decker, C.; Mayo, F. R.; Richardson, H. J. *Polym. Sci., Polym. Chem. Ed.* **1983**, *11*, 2879.
- (2) Fischer, H.; Hellwege, K. H.; Neudorfl, P. *J. Polym. Sci., Part A* **1963**, *1*, 2109.
- (3) Carlsson, D. J.; Dobbin, C. J. B.; Wiles, D. M. *Macromolecules* **1985**, *18*, 2092.
- (4) Plester, D. W. *Biomed. Eng.* **1970**, *5*, 443.
- (5) Dole, M. In *The Radiation Chemistry of Macromolecules*; Dole, M., Ed.; Academic Press: New York, 1972; Vol. 1, Chapter 14.
- (6) Geymer, D. O. In *The Radiation Chemistry of Macromolecules*; Dole, M., Ed.; Academic Press: New York, 1973; Vol. 2, Chapter 1.
- (7) Schnabel, W. In *Aspects of Degradation and Stabilization of Polymers*; Jellinek, H. H. G., Ed.; Elsevier: Amsterdam, 1978; Chapter 4.
- (8) Chatgililoglu, C.; Howard, J. A.; Ingold, K. U. *J. Org. Chem.* **1982**, *47*, 4361.
- (9) Chettur, G.; Snelson, A. J. *Phys. Chem.* **1987**, *91*, 913.
- (10) Carlsson, D. J.; Brousseau, R.; Zhang, C.; Wiles, D. M. *ACS Symp. Ser.* **1988**, No. 364, 376.
- (11) Carlsson, D. J.; Chmela, S.; Wiles, D. M. *Polym. Degrad. Stab.*, in press.
- (12) Atkinson, R.; Aschmann, S. M.; Carter, W. P. L.; Winer, A. M.; Pitts, J. N. *Int. J. Chem. Kinet.* **1984**, *16*, 1085.
- (13) Becker, R. F.; Carlsson, D. J.; Cook, J. M.; Chmela, S. *Polym. Degrad. Stab.* **1988**, *22*, 313.
- (14) Harrick, N. J. *Appl. Spectrosc.* **1977**, *31*, 548.
- (15) Hori, Y.; Shimada, S.; Kashiwabara, H. *Polymer* **1977**, *18*, 567.
- (16) Shimada, S.; Hori, Y.; Kashiwabara, H. *Macromolecules* **1988**, *21*, 979.
- (17) Gvozdic, N.; Basheer, R.; Mehta, M.; Dole, M. *J. Phys. Chem.* **1981**, *85*, 1563.
- (18) Beckwith, A. L. J.; Ingold, K. U. In *Rearrangements in Ground and Excited States*; de Mayo, P., Ed.; Academic Press: New York, 1980; Vol. 1.
- (19) Ranor, K. D.; Lusztyk, J.; Ingold, K. U. *J. Org. Chem.* **1988**, *53*, 5220.
- (20) Hegazy, E.-S. A.; Seguchi, T.; Arakawa, K.; Machi, S. *J. Appl. Polym. Sci.* **1981**, *26*, 1361.
- (21) Partridge, R. H. *J. Chem. Phys.* **1970**, *52*, 2485.
- (22) Tsuda, M.; Oikawa, S. *J. Polym. Sci., Polym. Chem. Ed.* **1979**, *17*, 3759.
- (23) Falconer, W. E.; Salovey, R. *J. Chem. Phys.* **1966**, *44*, 3151.
- (24) Howard, J. A.; Scaiano, J. C. In *Radical Reaction Rates in Liquids: Oxy-, Peroxy- and Related Radicals*; Fischer, H., Hellwege, K. H., Eds.; Springer-Verlag: Berlin, 1984 (Vol. 13 of Landolt-Bornstein New Series II, Part D).

**Registry No.** i-PP, 9003-07-0; PE, 9002-88-4; a-PP, 9003-07-0; CH<sub>3</sub>(CH<sub>2</sub>)<sub>10</sub>ONO<sub>2</sub>, 73377-37-4; CH<sub>3</sub>CH<sub>2</sub>CH(CH<sub>2</sub>ONO<sub>2</sub>)CH<sub>2</sub>CH<sub>3</sub>, 74398-55-3; CH<sub>3</sub>(CH<sub>2</sub>)<sub>4</sub>CH(ONO<sub>2</sub>)CH<sub>2</sub>CH<sub>3</sub>, 82944-62-5; CH<sub>3</sub>(CH<sub>2</sub>)<sub>7</sub>CH(ONO<sub>2</sub>)CH<sub>3</sub>, 129731-66-4; CH<sub>3</sub>CH(CH<sub>3</sub>)CH(ONO<sub>2</sub>)CH(CH<sub>3</sub>)CH<sub>3</sub>, 129731-67-5; CH<sub>3</sub>CH(CH<sub>3</sub>)CH<sub>2</sub>CH(ONO<sub>2</sub>)CH<sub>2</sub>CH(CH<sub>3</sub>)CH<sub>2</sub>CH(CH<sub>3</sub>)<sub>2</sub>, 129731-68-6; CH<sub>3</sub>C(CH<sub>3</sub>)<sub>2</sub>CH<sub>2</sub>C(CH<sub>3</sub>)<sub>2</sub>ONO<sub>2</sub>, 129731-69-7; CH<sub>3</sub>CH<sub>2</sub>C(CH<sub>3</sub>(ONO<sub>2</sub>)CH<sub>2</sub>CH<sub>3</sub>, 22083-39-2.